Journal of Nuclear Materials 382 (2008) 160–169

Contents lists available at ScienceDirect

Journal of Nuclear Materials

journal homepage: www.elsevier.com/locate/jnucmat

Microstructural defects in SiC neutron irradiated at very high temperatures

S. Kondo *, Y. Katoh, L.L. Snead

Materials Science and Technology Division, Oak Ridge National Laboratory, PO Box 2008, Oak Ridge, TN 37831-6138, USA

A B S T R A C T

Microstructures in high purity β-SiC irradiated with fast neutrons (up to ~9.6×10^{25} n/m^2, in HFIR) at very high temperatures (1130, 1300, and 1460 °C) were studied by transmission electron microscopy. Cavities and dislocation loops were generally observed in irradiated samples. The cavities were preferentially formed at grown-in stacking faults, and were spherical in shape below 1300 °C and mainly faceted with {1 1 1} planes at 1460 °C. Estimated volume fractions of observed cavities were much smaller than macroscopic densitometer swelling recently reported, which implies other defects cause the swelling in this temperature regime. Larger Frank loops (>25 nm in radius) formed at 1460 °C were identified as interstitial type using the inside/outside method. Unfaulting of the loops was not observed or was very rare. Rapid loop growth and density decrease were observed in the temperature range of 1300–1460 °C concurrently with the rapid cavity growth. The limited growth rate of dense loops at lower temperature was discussed in terms of high sink density estimated from a grain-boundary-loop-denuded zone formed at 1130 °C.

Published by Elsevier B.V.

1. Introduction

Recent interest in silicon carbide (SiC) and its composites has been motivated by its possible utilization as a structural material in nuclear energy systems [1]. The advantages include perceived radiation stability at temperatures <1000 °C that comes from retention of radiation produced nano-structured defects up to high fluences. The knowledge regarding the microstructural change in SiC during irradiation has thus far been mainly limited to the low-to-intermediate temperature regime, and has hampered the determination of upper temperature and fluence limits for the severe use conditions now being considered. Important rapid property changes are anticipated at very high temperatures, where irradiation induced microstructural defects undergo unstable growth. Our recent study has focused on the evolutions of dislocation and void microstructures in neutron-irradiated β-SiC, especially for the high temperatures beyond the upper service temperature limits for metallic heat resistant structural alloys.

The literature offers only limited microstructural information on β-SiC subjected to high temperature neutron irradiation. Price [2] first observed irradiation induced void formation in SiC deposited on graphite discs, the irradiation condition of void formation was neutron fluence of 4.3×10^{25} n/m^2 ($E > 0.18$ MeV) and an irradiation temperature of 1250 °C or higher. Several self-ion irradiation experiments also reported cavity formation in CVD SiC, where cavities were observed at >1000 °C [3]. No other information on void microstructures in neutron-irradiated β-SiC has been available. Price [4] and Blackstone and Voice [5] reported macroscopic volumetric expansion in neutron irradiated SiC at high temperatures (~1500 °C). Recently, Snead et al. [6,7] reported the temperature and fluence dependent swelling in CVD SiC in the high temperature regime, and formation of voids was considered the probable cause of the swelling.

Other microstructural features in neutron-irradiated SiC are black spot defects and/or small dislocation loops ($r \sim 3$ nm) after irradiation at relatively low fluences between 300 and 1100 °C [2,8–13]. The small dislocation loops were identified as lying on {1 1 1} lattice planes [2], and have been tentatively identified as Frank loops without Burgers vector analysis. Recently, Katoh et al. [13] suggested that these were a mixture of Frank loops and other type defect clusters, for example having Burgers vector of Shockley partial, by means of Burgers vector analysis for CVD SiC irradiated to 7.7×10^{25} n/m^2 ($E > 0.1$ MeV) at 800 °C. No evidence was reported because of their small size, but these defects were believed to be interstitial type based on difference in the mobilities of interstitials and vacancies in SiC. A high-resolution electron microscope image of a relatively larger planner defect on (1 1 1) in heavy-neutron irradiated SiC has been estimated to be an interstitial-type Frank loop by image simulation [14,15]. The formation of dislocation networks at 1400 °C in a self-ion irradiation experiment with well-controlled irradiation conditions was reported [13]. However, no neutron-irradiation effects on the dislocation microstructure at very high temperature (>1100 °C) have been reported.

* Corresponding author. Tel.: +1 865 576 6301; fax: +1 865 241 3650.
E-mail address: kondos1@ornl.gov (S. Kondo).

0022-3115/$ - see front matter Published by Elsevier B.V.
doi:10.1016/j.jnucmat.2008.08.013

It is noted that some of these earlier work of neutron-irradiated SiC, while valuable, likely contained uncertainty in critical irradiation conditions and unexpected effects of preexisting pores and impurities in old specimens [16].

This work presents initial results of a systematic study of microstructures in high purity β-SiC samples, obtained following neutron irradiation for a wide range of temperature (1130–1460 °C) and fluence (~9.6×10^{25} n/m^2). Of importance is that both the irradiation fluence and temperature were well characterized for this experiment.

2. Experimental

The material used for this work was poly crystalline β-SiC which was produced by chemically vapor deposition by Rohm and Haas Advanced Materials (Woburn, Massachusetts) [17]. The CVD material is extremely pure, with typical total impurity concentration of less than 5 wppm. The grain size is between 5 and 10 μm in the plane parallel to the deposition substrate, with the grains elongated in the <1 1 1> growth direction perpendicular to the substrate. The material is typically free of microcracks or other large flaws, but atomic layer stacking faults on the {1 1 1} planes are common. There is no porosity in CVD SiC, and the material is generally considered to be of theoretical density (approximately 3.21 g/cm^3).

Three fixed-core capsules, each containing 10 sub-capsules, were irradiated in the high flux isotope reactor at Oak Ridge National Laboratory at the temperatures of 1130, 1300, and 1460 °C. The highest fluence for the specimen studied here was 9.6×10^{25} n/m^2 corresponding to 9.6 SiC-dpa ($E > 0.1$ MeV). Irradiation conditions for each specimen are listed in Table 1. Irradiation temperatures were estimated by post-irradiation examination of melt wires inserted in both ends of each sub-capsule, and the uncertainty of the irradiation temperature was approximately ±85 °C averaged for these specimens. Detailed irradiation conditions were described elsewhere [6].

Specimens of 5.8 mm diameter with 0.5 or 3.2 mm thickness were axially cut in thin strip and mechanically polished to

Table 1
Microstructural defect parameters for neutron irradiated β-SiC

Irradiation temperature (°C)	Fluence ($E > 0.1$ MeV) $\times 10^{25}$ n/m^2	Cavity			Loop	
		Number density (m^{-3})	Size[a] (nm)	Calculated volume fraction	Number density (m^{-3})	Radius (nm)
1130	1.5	1.8×10^{20}	1.1	4.3×10^{-8}	9.1×10^{22}	2.2
1130	7.7	1.7×10^{21}	1.1	6.2×10^{-7}	9.2×10^{22}	4.1
1300	5.3	2.7×10^{23}	1.2	9.6×10^{-5}	5.4×10^{22}	6.3
1460	1.9	3.6×10^{22}	3.0	1.3×10^{-4}	4.0×10^{21}	16
1460	5.8	6.9×10^{22}	4.5	1.1×10^{-3}	1.2×10^{21}	28
1460	9.6	6.6×10^{22}	5.7	2.4×10^{-3}	3.7×10^{20}	43

[a] Diameter for cavities in spherical shape and side length for near 'triangular' voids were measured and averaged.

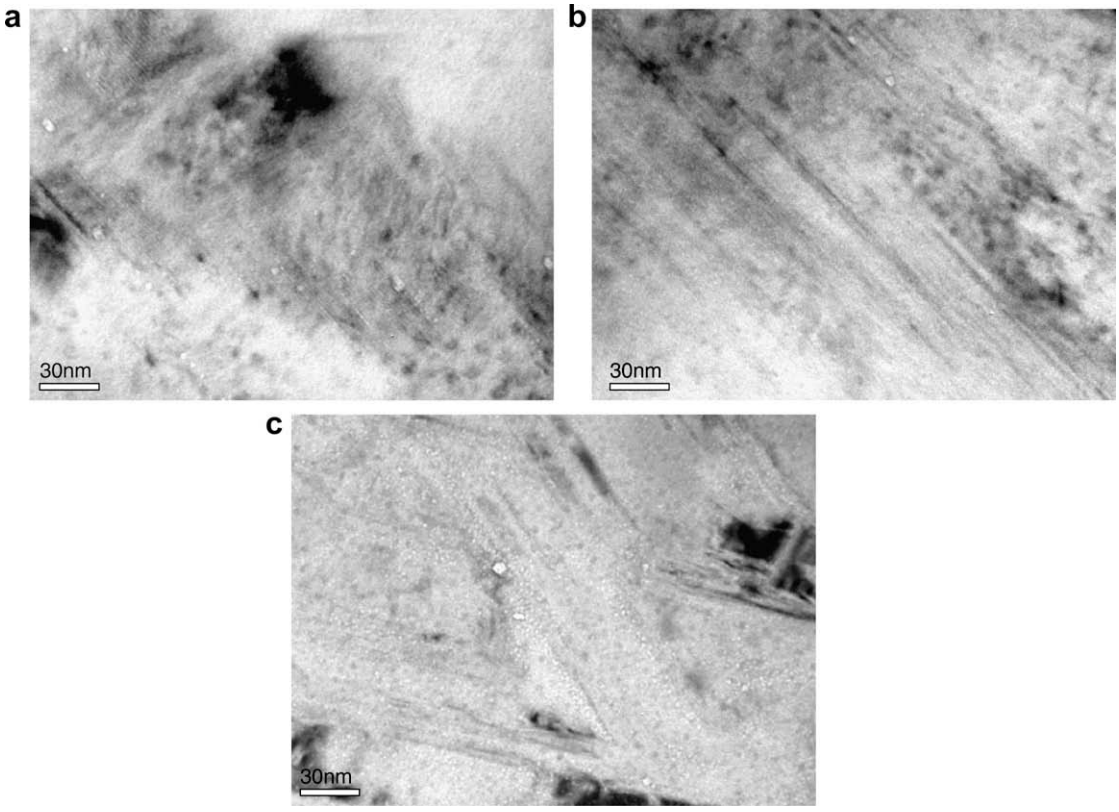

Fig. 1. Preferential nucleation of cavities on stacking faults in highly faulted grain in β-SiC irradiated at (a) 1130 °C, 1.5×10^{25} n/m^2, (b) 1130 °C, 7.7×10^{25} n/m^2, and (c) 1300 °C, 5.3×10^{25} n/m^2.

~30 μm thickness. Thin foils were prepared in a commercial Ar-ion-milling unit (FISCHIONE model 1010) using 3–5 keV dual ion beam. Microstructures were studied using a transmission electron microscope (Philips/FEI Technai 20, 200 keV).

3. Results

3.1. General microstructural features in unirradiated and irradiated SiC

In an unirradiated specimen no dislocation loops, pores, or precipitates were observed, but dense twin bands and stacking faults were heterogeneously distributed in some grains. Selected area diffraction patterns of the unirradiated specimen revealed that all the observed grains had the cubic structure, and this lattice structure was maintained after irradiation. In the specimens irradiated below 1300 °C, dislocation loops and small cavities were observed; in addition, faceted voids were observed at 1460 °C. The size and number densities of these defects are summarized in Table 1. Initial microstructural features, such as the dense faults, might slightly affect quantitative analysis of the irradiation induced defects at the locations. Therefore, multiple (more than three) TEM micrographs obtained from different crystal grains were used for the quantitative analysis to eliminate large contributions of the localized inhomogeneities. Although microstructural features with substantial electron transparency difference from the SiC matrix were observed at 1460 °C, the microstructural features or related pits formed at the foil surface have not yet been analyzed.

3.2. Cavity microstructure

Fig. 1 shows cavities in SiC irradiated at 1130 °C for (a) and (b), and 1300 °C for (c). Irradiation fluences are provided in the caption. The cavities were imaged under both kinematical underfocus and overfocus conditions to identify small cavities, the underfocused images are shown in the figure. Very sparse cavities were observed only in highly twined or faulted grains in SiC irradiated at 1130 °C as shown in the Figs. 1(a) and (b). These images do not represent the general microstructure, but show the selected grains which contain many cavities, i.e., the cavity microstructure strongly related to the initial microstructures such as density of stacking faults. Visible cavities were not detected in the matrix without stacking faults, and a number of stacking faults without cavity were also observed at 1130 °C. At 1300 °C (Fig. 1c), very small, dense cavities were generally observed in the faulted planes. The number densities of the visible cavities were strongly dependent on both the irradiation temperature and fluence as shown in Table 1.

Fig. 2 shows the cavities (small cavities in spherical shape and faceted voids) formed at 1460 °C, the irradiation fluence are 1.9×10^{25} n/m^2 for (a), 5.8×10^{25} n/m^2 for (b) and (c), 9.6×10^{25} n/m^2 for (d), respectively. Spherical cavities and several polygonal, essentially triangular shape in projection to the viewing plane, voids were observed at 1.9×10^{25} n/m^2. Figs. 2(b) and (c) are the same specimen and were taken near $B = [1\,1\,1]$ and $[0\,1\,1]$, respectively. In Fig. 2(b), two sides of the 'triangular' voids parallel to $(1\,\bar{1}\,1)$ and $(1\,1\,\bar{1})$ planes, respectively, while the other side is parallel to $[0\,2\,\bar{2}]$ direction. Many voids are truncated at both ends of

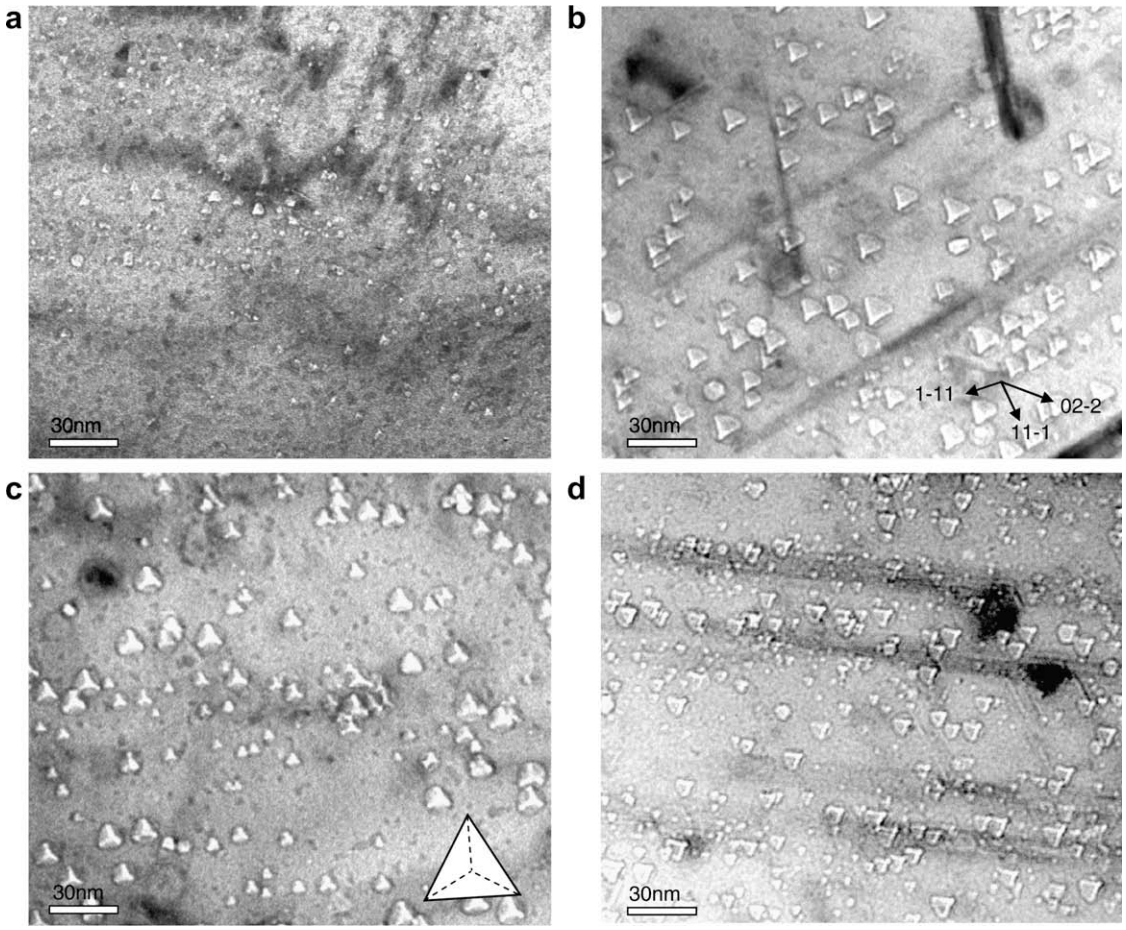

Fig. 2. Faceted voids in β-SiC irradiated at (a) 1460 °C, 1.9×10^{25} n/m^2, (b, c) 1460 °C, 5.8×10^{25} n/m^2, and (d) 1460 °C, 9.6×10^{25} n/m^2. The beam axis are B ~ 0 1 1 for (a), (b) and (d) B ~ 1 1 1 for (c).

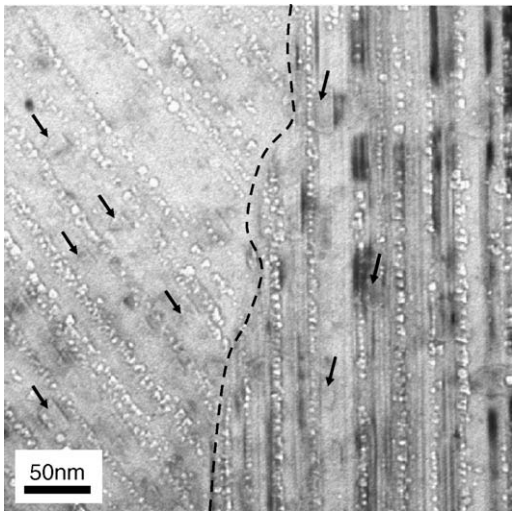

Fig. 3. Preferential nucleation of faceted voids in β-SiC irradiated to 5.8×10^{25} n/m^2 at 1460 °C. The beam axis is $B \sim 110$ for left grain. Unanalized defects and/or related pits are indicated by arrows. Dotted line indicates a grain boundary near parallel to electron beam direction.

the side parallel to [02$\bar{2}$]. Very few hexagonal voids were also observed in the specimen. It is noted that all the 'triangular' voids formed in the same grain are oriented in the identical direction as shown in Fig. 2(b). Different features of the voids can be seen in Fig. 2(c). Three white lines in the voids were imaged, and the excited line-contrasts appeared parallel to three <112> direction indicated by dotted lines in the inset Thompson's tetrahedron, respectively.

Cavities formed in matrix regions without stacking faults become common at 1460 °C, but the preferential formation of the smaller voids at stacking faults are also observed. Typical example

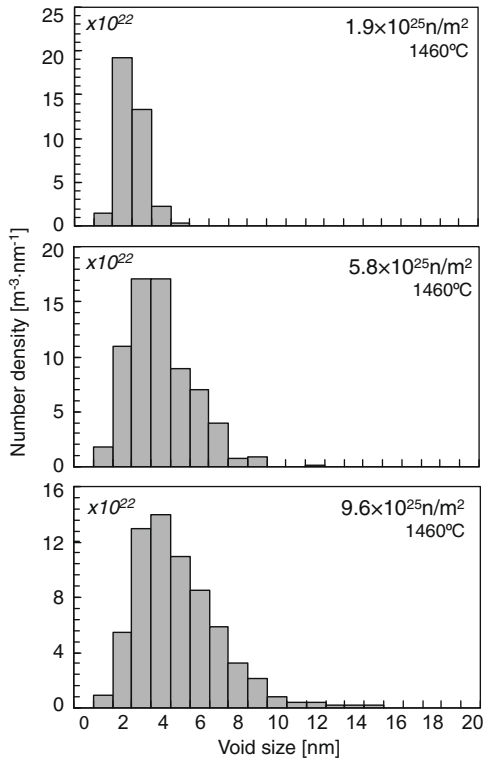

Fig. 4. Size distributions of faceted voids in β-SiC irradiated up to 9.6×10^{25} n/m^2 at 1460 °C.

of the voids aligned with {111} planes in SiC irradiated to 5.8×10^{25} n/m^2 at 1460 °C is shown in Fig. 3. A grain boundary extending from top to bottom of the image is seen in the figure indicated by a dotted line. There is no preferential formation of cavities on the grain boundary. The grain on the left was taken from near 110 axis, and the faulted planes were viewed approximate edge-on. The number density of voids formed between the faulted planes are apparently lower than voids formed on faulted planes. Unanalyzed microstructural features showing weak contrast are indicated by arrows in Fig. 3.

The size distribution of the cavities in SiC irradiated to 1.9, 5.8, and 9.6×10^{25} n/m^2 at 1460 °C are presented in Fig. 4, respectively. Although the resolution limit for cavities was approximately 1 nm in this study, it is likely that cavities smaller than 1 nm are present in substantial concentrations. This implies that the number densities of smaller cavities were probably underestimated. An increase in the mean size with increasing fluence is observed (see Table 1), which is attributed primarily to the spreading at the larger-side of the size distribution. The small cavity density remains high even at the highest fluence of 9.6×10^{25} n/m^2.

3.3. Dislocation loop microstructure

Fig. 5 shows the microstructures in SiC irradiated at 1130 °C for (a) and (b), and 1300 °C for (c). Each image is from the same specimen as shown in Fig. 1, respectively. Loop size and number densities listed in Table 1 were measured by corresponding weak-beam dark field (WBDF) images, since the small loops were difficult to image under bright field (BF) imaging condition. The loops were seen to be edge-on under the imaging condition of [011] beam axis with g = [022] reflection. From $g \cdot b$ contrast analysis, most loops formed at 1130 °C have Burgers vector parallel to <111>, or at least perpendicular to one of <220> directions on their loop planes. At 1300 °C, relatively larger loops were observed at 5.3×10^{25} n/m^2, and their Burgers vectors were confirmed to be perpendicular to the each loop plane. Additionally, extended diffraction streaks (111 rel-rod streaks), which confirmed to be arising from the edge-on loops, were detected except for Fig. 5(a). The fluence dependent loop density at 1130 °C was almost saturated at 1.5×10^{25} n/m^2 (see table. 1), and it decreased with irradiation temperature. The loop size increased with increasing irradiation temperature and fluence.

Fig. 6 shows the WBDF images of SiC irradiated at 1460 °C, the irradiation fluence are 1.9×10^{25} n/m^2, 5.8×10^{25} n/m^2, and 9.6×10^{25} n/m^2, respectively. Images were taken from close to [111] for (a) and close to [112] for (b) and (c) under g = 220 condition, where loops formed on two different {111} planes can be imaged. Residual contrast associated with Frank loops formed on other two planes could be ignored in Fig. 6(a) because of the weak image contrast. The loops in image (a) give the appearance that those are polygonal shape consisting of the dislocation segments parallel to <110> directions.

At the fluence of 5.8×10^{25} n/m^2 at 1460 °C, the loop size become comparable to, or exceeds the foil thickness. Fringe contrasts in Figs. 6(b) and (c) are consistent with identification of the loops as larger Frank faulted loops, though the complete image of the loops could not be obtained because of their larger size. A number of dislocations with b//<111>, those were likely the loop edges, were also detected in these specimens. Larger Frank loops embedded between existing stacking faults are hardly distinguishable from the pre-existing faults, and overlapped faults could not be analyzed clearly by conventional TEM techniques. We measured the size and number density of only edge-on loops imaged from loop related {111} relrods on their <011> diffraction pattern, which provide relatively precise information about their size. However, the measured loop size and density for the specimens

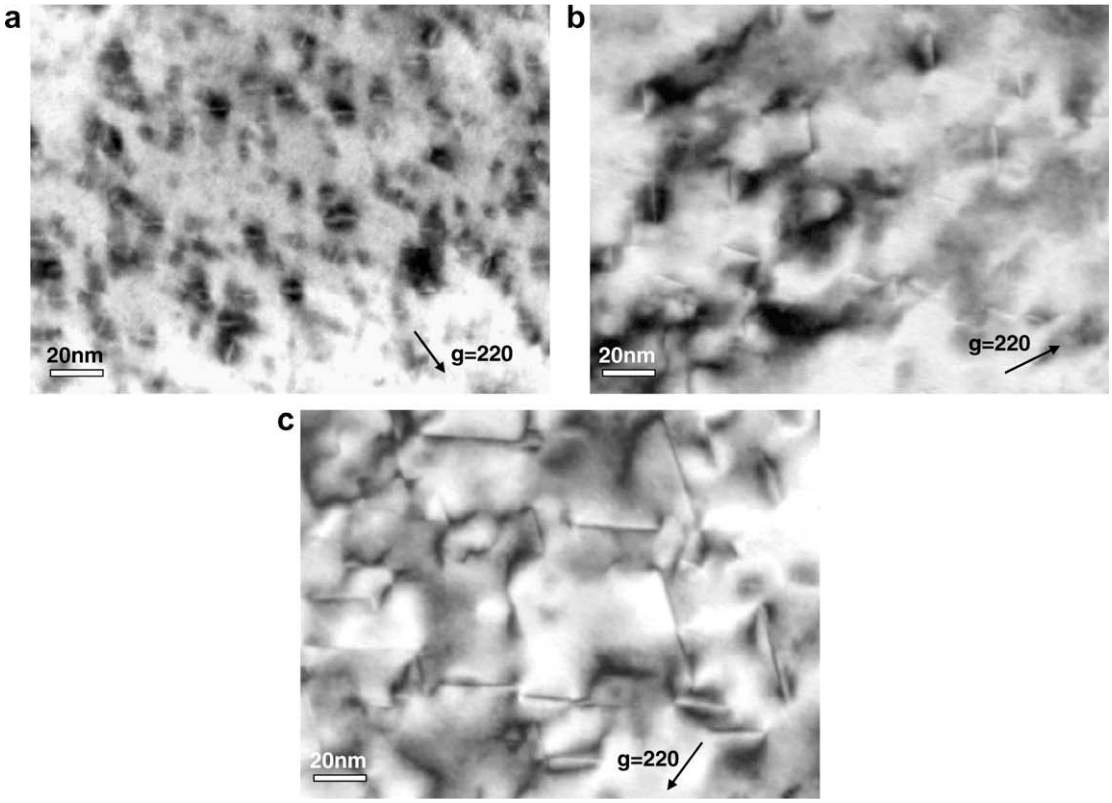

Fig. 5. Dislocation loops formed on {1 1 1} family in β-SiC irradiated at (a) 1130 °C, 1.5×10^{25} n/m^2, (b) 1130 °C, 7.7×10^{25} n/m^2, and (c) 1300 °C, 5.3×10^{25} n/m^2 as in Fig. 1.

irradiated to 5.8×10^{25} n/m^2 and 9.6×10^{25} n/m^2 at 1460 °C listed in Table 1 may contain large errors for the reasons stated above. Although some dislocation segments with Burgers vector parallel to <1 1 0> or <1 1 2> were observed, these are not the dominant microstructure. The Burgers vectors are most probably $a_0/2$<1 1 0> and $a_0/6$<1 1 2> which are perfect dislocation and Shockley partial dislocation, respectively. However, the unfaulting process of Frank loops seems to occur less frequently under the conditions studied here. The bright contrast in the shape of dots or loops (<∼10 nm) in Figs. 6(b) and (c) were confirmed to arise from the voids and unknown microstructural features by means of comparison with equivalent BF images.

The result of inside/outside analysis [18] to determine the vacancy/interstitial nature of the loops observed in SiC irradiated to 1.9×10^{25} n/m^2 at 1460 °C is presented in Fig. 7. These were taken close to $B = [1\,1\,1]$ under $2\,0\,\bar{2}$ (for the left image) and $\bar{2}\,0\,2$ (right image) weak-beam conditions, respectively. Corresponding Thompson's tetrahedron and Kikuchi patterns around the 111 pole are illustrated in the figure. The loop planes can be determined by considering the stacking fault fringes and change in its projection width at the known tilt. The loop planes were shown in the schematic image. In the right TEM image, the loops show inside-contrast for loops (a) and (c), outside-contrast for loops (b) and (d). In the left TEM image, the inside/outside contrast are reversed. Considering the rotation of the diffracting planes at the edge of loops and the sign of the deviation parameter used here (S_g>>0), the four analyzed loops are determined to be interstitial type loops.

4. Discussion

4.1. Cavity microstructure

Senor et al. [12] reported the absence of cavities in β-SiC irradiated to 0.9×10^{25} n/m^2 at 1100 °C, whereas cavities are observed following subsequent annealing at 1500 °C for 1 h. In contrast, the present results showed the cavity formation at 1130 °C and fluence dependent increase of the density. The cavity formation at ∼1100 °C is supposed to be likely [13] because silicon vacancy in SiC starts to migrate at 800–900 °C as described elsewhere [19,20]. However, the mean cavity size at higher fluence was retained at 1.1 nm which was still comparable to cavity resolution limit, that is, the growth rates of the cavities were very limited and the cavity swelling were negligible as discussed below.

The present results of quantitative analyses of cavities were somewhat different from the earlier report in comparable irradiation conditions [2]. The cavity density ($N_C = 2.7 \times 10^{23}$ m^{-3}) observed at 5.3×10^{25} n/m^2, 1300 °C is somewhat higher than the previous reported ($N_C = 1.4 \times 10^{23}$ m^{-3}) at 4.3×10^{25} n/m^2 ($E > 0.18$ MeV), 1250 °C [2]. Also, the mean cavity size observed here ($d_C = 1.6$ nm) is less than half of the previous report ($d_C = 3.5$ nm). Price has stated that the cavity size resolvable with certainty was larger than 3 ∼ 4 nm, therefore, the disagreements are primary due to the larger analytical errors for the small cavities in the earlier work. It has also been stated in [2], that most cavities at 1250 °C had facets, while cavities observed in this work were roughly spherical at 1300 °C. This implies that the irradiation temperature of the previous work was somewhat higher than the present work, and/or the initial material conditions such as impurities in the old SiC specimens modified the cavity microstructure. The size and number densities of cavities formed at 1460 °C were also slightly different from previous results at 1500 °C [2], likely for similar reasons. On the other hand, the cavity size distribution showed a similar trend to the previous report for the nucleation- and growth-behavior as shown in Fig. 4. It has been concluded in his report that both the nucleation and growth continued to high fluence at 1500 °C.

Near tetrahedral voids with {1 1 1} facets have also been reported for β-SiC irradiated at 1500 °C by Price [2], but detailed

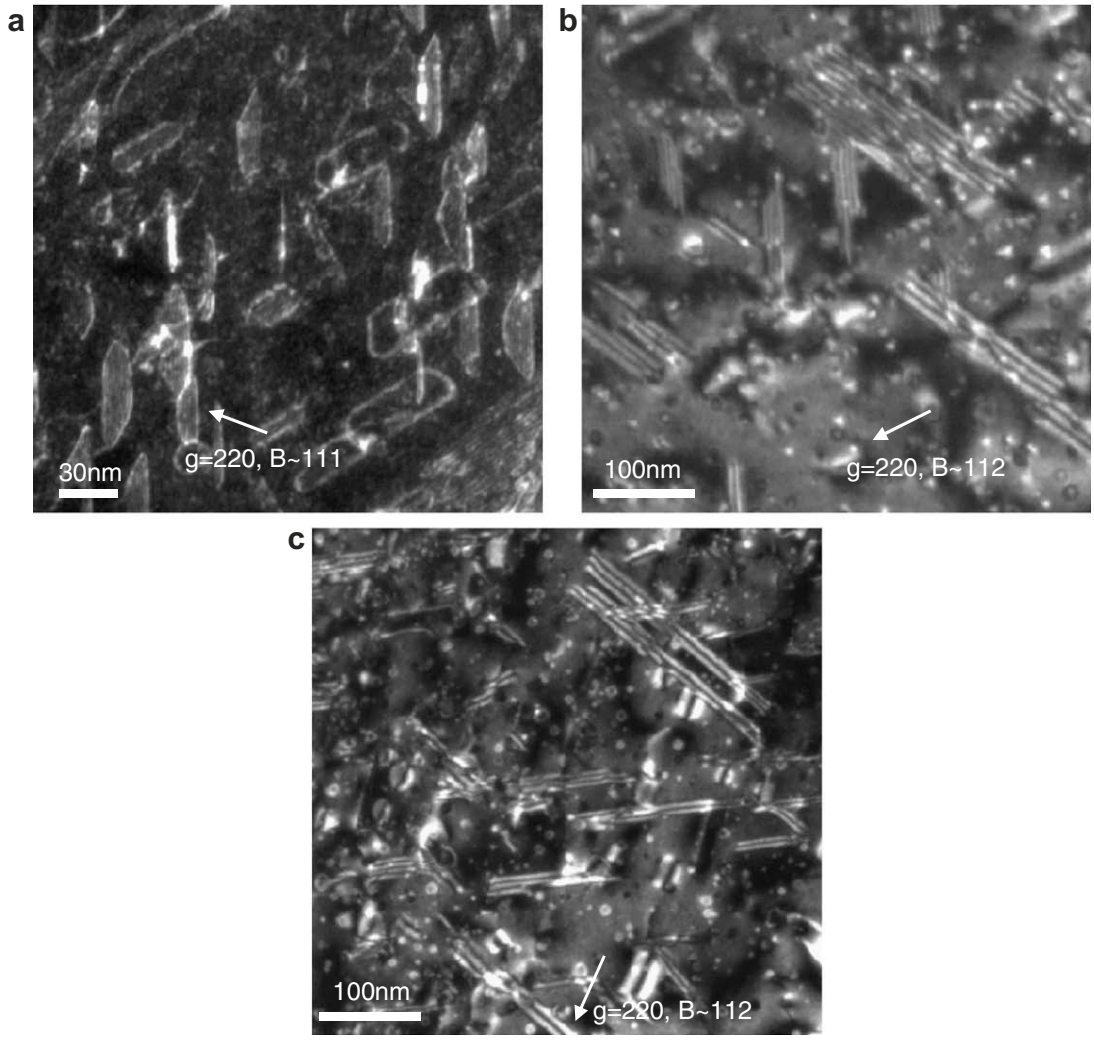

Fig. 6. Weak-beam dark field images of Frank loops formed in β-SiC irradiated at (a) 1460 °C, 1.9×10^{25} n/m^2, (b) 1460 °C, 5.8×10^{25} n/m^2, and (c) 1460 °C, 9.6×10^{25} n/m^2.

analysis of the faceted surfaces was not included. A regular tetrahedral void, for example, has 49% more surface area than a spherical void for a given volume, meaning free surface energy of the faceted surfaces is much lower than that of other surfaces. The {1 1 1} facets are commonly reported for voids in Si with tetrahedrally coordinated covalent crystal with diamond structure, and the {1 1 1} family was experimentally estimated to the most stable free surface in Si [21,22]. However, the void shape in Si is not tetrahedron but {1 1 1} octahedron truncated with {1 0 0} facets. Considering the results of Figs. 2(b) and (c), the dominating three dimensional structure of voids observed here is most probably tetrahedral, truncated at the corners with {1 1 1} facets. Additionally, low index surfaces such as {0 1 1} and {0 0 1} were not observed in the present magnification range even in the specimen irradiated to 9.6×10^{25} n/m^2 at 1460 °C. These results suggest that the {1 1 1} lattice planes have the lowest surface energy in β-SiC as previously estimated by Givargizov [23]. Since the helium production rate in SiC under HIFR irradiation was calculated to be 2.5 appm He/dpa [24], the accumulated helium might stabilize the nucleation and early stage of accumulation of vacancies. This is probably one of the reasons that mainly spherical small cavities are observed for the conditions of lower fluence and temperatures. However, the dominance of faceted voids suggests that the observed cavities and voids are underpressurized and grow by a bias-driven growth mechanism.

Preferential formation of cavities and voids at stacking faults were observed in all irradiated specimens. Indeed, Price has previously reported this tendency in SiC irradiated at 1250 °C and 1500 °C, and suspected it was caused by impurities segregated at faults [2]. However, it is not applicable to the specimens used here because of their highly-pure chemical composition. Stacking faults and twin boundaries in this system are irregular stacking sequence of tetrahedrally bonded Si–C bilayer without breaking of bonds or grain boundary dislocations, where there is little disturbance of the structure. Furthermore, several theoretical calculations even implied negative stacking fault energies for β-SiC [25–28]. Therefore, stacking faults in β-SiC do not seem to be either significant sources or sinks for point defects. Nevertheless, most of the small cavities were observed at stacking faults in the specimens irradiated below 1300 °C, indicating the preferential cavities nucleation at or very close to the stacking faults. When the stacking fault energy is negative, surface creation at the faulted plane will be energetically unfavorable. The observation, therefore, supports that β-SiC has positive stacking fault energy, and cavity formation at the faulted plane could reduce the free energy increment.

4.2. Cavity swelling

Cavity volume fractions including previously reported data are plotted in Fig. 8. The volumes of the faceted voids were estimated

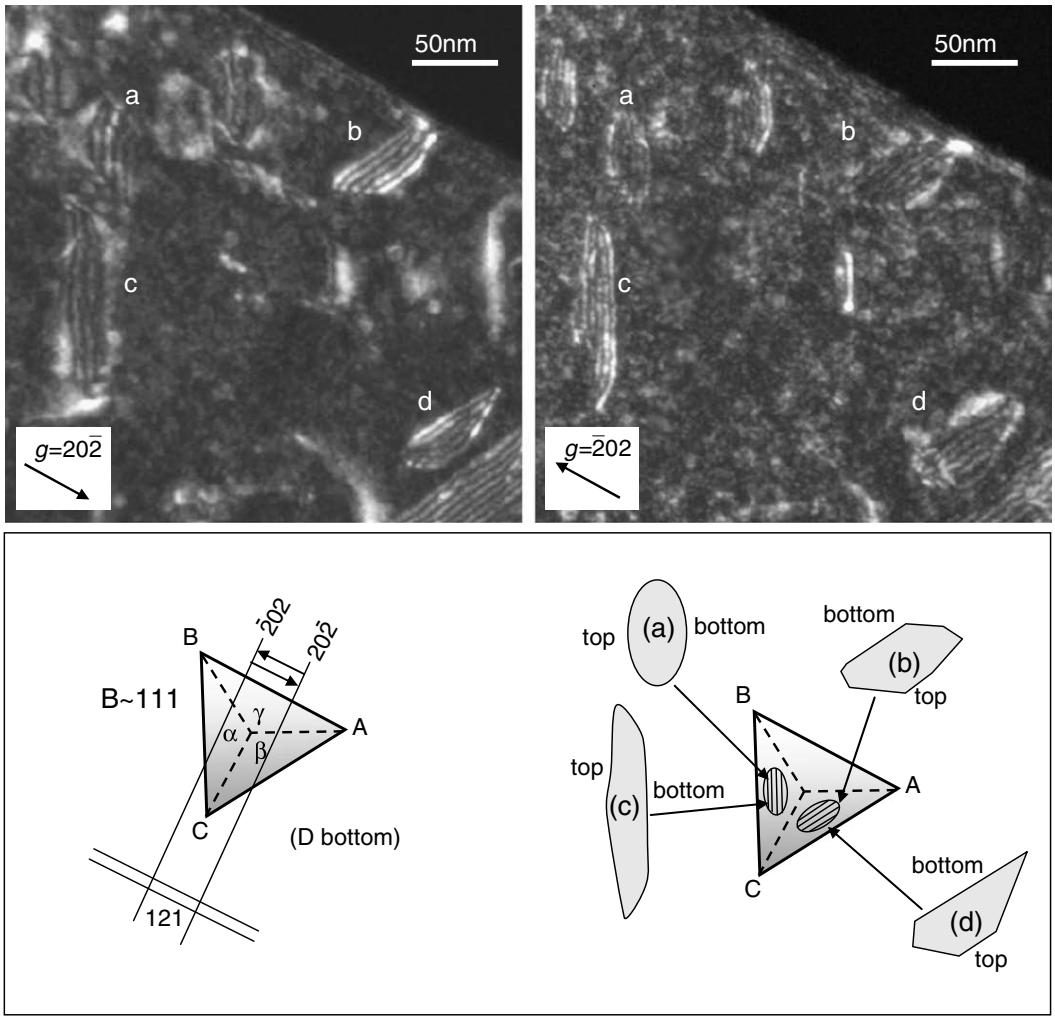

Fig. 7. Inside/outside-contrast analysis of Frank loops formed in β-SiC irradiated to 1.9×10^{25} n/m^2 at 1460 °C. The inside/outside-contrast of the loops are reversed under the opposite sign of g vector. These loops are determined to be of interstitial type.

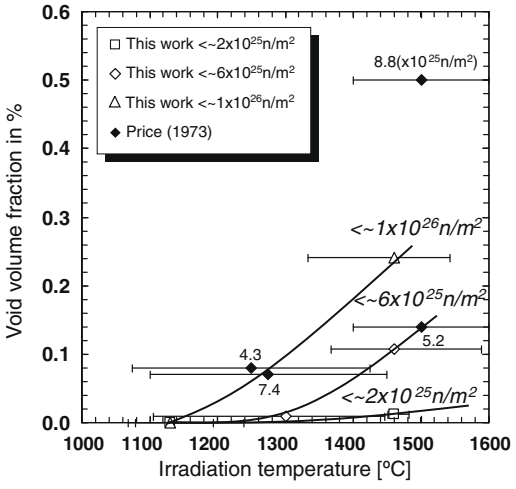

Fig. 8. Irradiation temperature dependence of cavity volume fraction for neutron-irradiated β-SiC.

assuming regular tetrahedron shape, in the same way as by Price [2]. The volume fraction increased with increasing fluence and irradiation temperature without a peak. The lowest temperature, where unsaturatable swelling occurs, was reported to be 1100 °C, based on densitometry [6]. The absolute values of the estimated void fractions, however, are lower than the macroscopic densitometer swelling values by a factor of <~10. The lower temperature limit for cavity swelling is important for determining irradiation limits of structural material; swelling saturates at lower temperatures as a result of saturation of point defects and point-defect clusters, whereas it is not likely to saturate when swelling is driven by cavities [2,4,5,29–31]. The lowest temperature at which void formation previously reported was ~1250 °C [2]. Whereas, sparse cavity populations were observed at 1130 °C, the volume fractions of these cavities were estimated to be $<10^{-6}$. Thus, the observed cavities in these specimens can not be the primary cause of the macroscopic swelling [6]. The possible explanation of the discrepancy between the void fraction and the macroscopic swelling is the existence of a large number of tiny defects such as invisible cavities (or vacancy clusters) and/or other kinds of defects. For example, the isolated anti-site defects, which are likely to be stable at high temperature due to very high formation energy of interstitials [32], could contribute to the lattice expansion [33].

4.3. Dislocation loops

The dominant dislocation microstructure component in the irradiated specimens studied here is dislocation loops, presumably

of interstitial type. At 1130 °C, the loop density seemed to be saturated at the value of $\sim 9 \times 10^{22}$ m^{-3} at 1.5×10^{25} n/m^2, but the size increased with fluence. The negative temperature dependence of loop density and positive temperature dependence of loop radius are well supported by the results of self-ion irradiation experiments [13]. Almost linear fluence dependent growth was observed at 1460 °C, where the loop growth rate was more than 10 times higher than that at 1130 °C. The decrease in loop population with increasing fluence at 1460 °C might indicate the coalescence of adjoining loops and/or vacancy absorption at the loops. The interference of the Frank faulted loops is known to trigger an unfaulting process of the faulted plane in metals [34,35]. However, the absence of perfect loops with $b = a_0/2\langle 1\,1\,0\rangle$ in the specimen implies the quite low extrinsic stacking fault energy in SiC. One can conclude that the Frank loops are extremely stable configuration of interstitial clusters in β-SiC in the high temperature regime (>∼1000 °C). The most stable configuration of perfect loops and related networks may be formed under the condition of higher temperature and fluence as demonstrated in self-ion irradiated SiC [13].

Fig. 9 shows both the WBDF and BF images of the loops adjacent to a grain boundary for (a) and to stacking faults for (b) in SiC irradiated to 1.5×10^{25} n/m^2 at 1130 °C. Loop denuded zone (DZ) along the grain boundary (∼20 nm in width) is shown in Figs. 9(a) and (a′), in contrast, there is no evident zone of loops denuded at the stacking faults in Figs. 9(b) and (b′). A defect-free zone with much lower loop density exists along grain boundaries has been often observed in irradiated metals and ceramics [36,37], and the underlying mechanisms have been well understood by kinetic equations with diffusion terms [38–41]. No grain-boundary DZ of either the black spots or loops has been reported in neutron-irradiated SiC. In this temperature regime, pseudo-steady state concentrations of point defects in matrix are dependent primary on the sink strength. Assuming that all the loops are of interstitial type and corresponding vacancies form three-dimensional clusters (cavities), the ratio of sink strength of cavities to that of loops is $k_C^2/k_L^2 \approx 3r_L b/2r_C^2 \gg 1$, where r_L is the mean loop radius, r_C is the mean cavity radius, and b is the Burgers vector. The total sink strength, therefore, related primarily to the sink strength of the TEM invisible cavities. Because the difference in capture efficiency of the cavities for interstitials and vacancies are generally small, the assumption of $k_{C,i}^2 = k_{C,v}^2$ may be acceptable, where $k_{C,j}^2$ is the sink strength of the 'invisible' cavities for j species. The loop denuded width, thus, can be roughly estimated as $l_L^2 \approx 1/k_{C,v}^2$, when the width is small enough and the loop distribution is almost independent from the distance from the grain boundary outside the DZ. The number density and mean diameter of the 'invisible' cavities in the specimen irradiated to 1.5×10^{25} n/m^2 at 1130 °C were

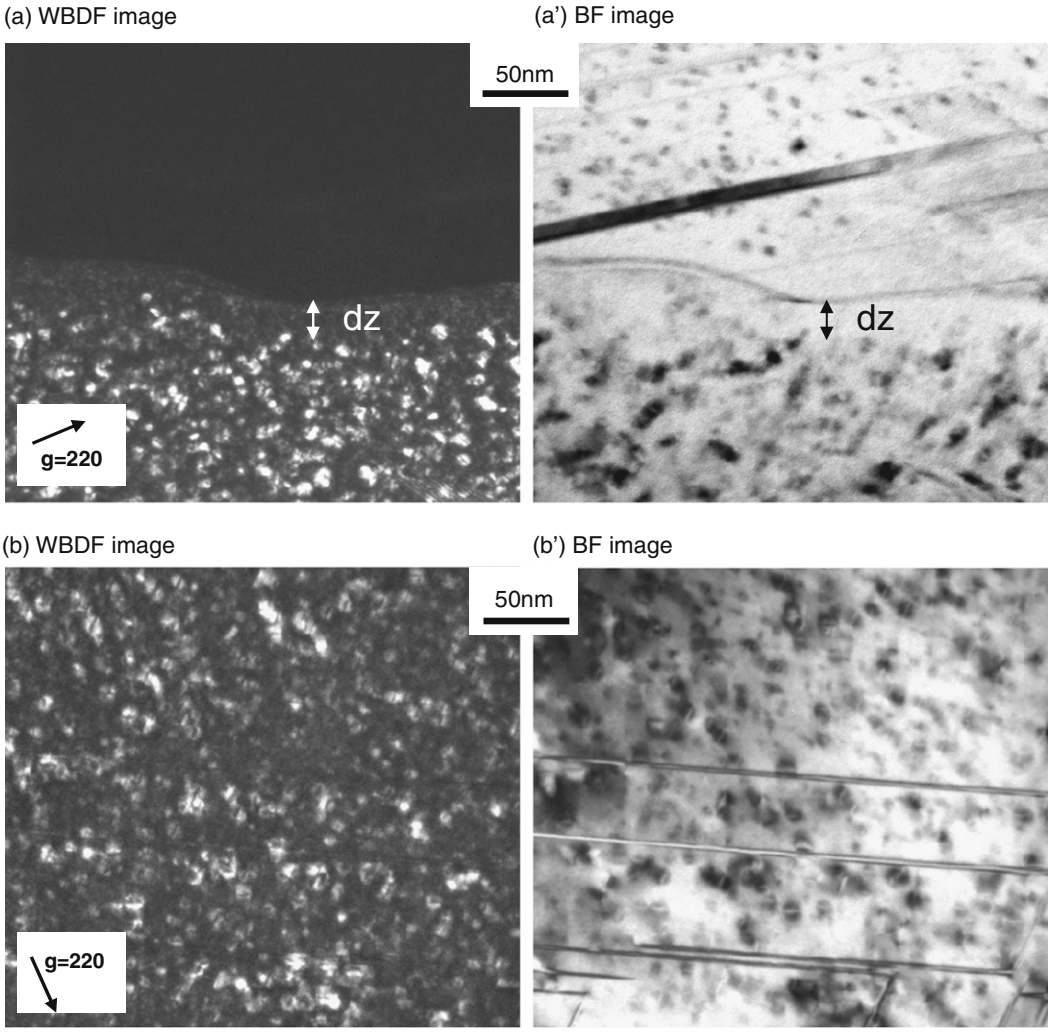

Fig. 9. (a), (a′) Denuded zone (dz) for dislocation loops along grain boundary in β-SiC irradiated to 1.5×10^{25} n/m^2 at 1130 °C. (b), (b′) Loop images near stacking faults in the same specimen without the evident of 'dz'.

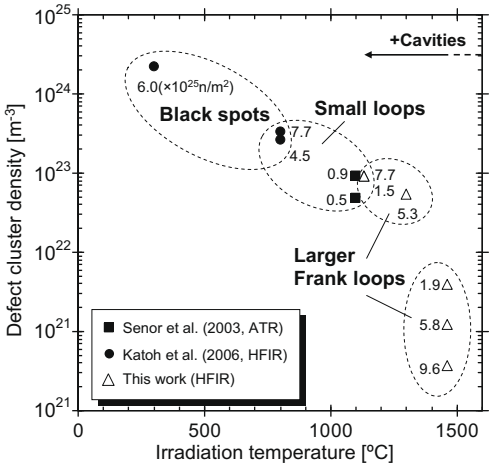

Fig. 10. Irradiation temperature dependence of defect cluster densities in neutron irradiated β-SiC. Black spots (defect clusters with unidentified configuration), Small loops (loops with various Burgers vectors), and Larger Frank loops (identified by 1 1 1 streaks or $g{\cdot}b$ analysis) are included in the defect clusters.

roughly estimated to be $\sim 3 \times 10^{23}$ m^{-3} and $\sim$1 nm, respectively. It is to note that the obtained values are reasonable, which implies being of a great number of TEM invisible cavities nearly comparable in size to the cavity resolution limit. This result also supports that the most of observed loops are interstitial type.

Fig. 10 shows the irradiation temperature dependence of number density of defects including black spots with various indeterminate configurations [13], small loops with various Burgers vectors [12,13], and larger Frank loops. Defect density decreased with increasing irradiation temperature, where the rapid decrease was observed at 1300–1460 °C. At 1460 °C, loops grow rapidly and develop into larger Frank loops concurrently with the formation of faceted voids. The loops in SiC, which is somewhat an ionic compound, should maintain their stoichiometric structure [42,43]. The influx of Si interstitials has been pointed out as a parameter responsible for controlling the loop growth [44]. However, the influx might be limited due to the annihilation of interstitials at the vacancy clusters under the condition where the TEM invisible cavities dominate the sink strength for point defects. Therefore, above the temperature where the mobility of vacancies is significant, the reduced sink strength presumably allows the rapid decrease of loop density and rapid loop growth.

5. Summary

Defect microstructures of polycrystalline CVD SiC irradiated with fast neutrons (up to $\sim 9.6 \times 10^{25}$ n/m^2) at very high temperatures (1130–1460 °C) were analyzed using transmission electron microscopy. Irradiation-induced cavities, voids, and dislocation loops were identified at all irradiation temperatures.

The cavities were predominantly spherical in shape below 1300 °C. Additional voids faceted with {1 1 1} planes were dominating at 1460 °C, which were basically tetrahedral truncated at the corners with {1 1 1}. Small cavities were dispersed with low number density in highly faulted grain at 1130 °C. Preferential formations of cavities at stacking faults were confirmed above 1300 °C, namely the grown-in stacking faults greatly affected both the local cavity size and number density. Volume fraction of the cavities increased dramatically at 1460 °C. The cavity volume fraction estimated to be 2.4×10^{-3} at 9.6×10^{25} n/m^2 at 1460 °C was much lower than the macroscopic densitometry swelling previously reported. This indicates that those visible cavities were not the main cause for high temperature swelling.

With increasing irradiation temperature, the size of dislocation loops increased and the number density decreased. Large dislocation loops formed at 1460 °C were identified as interstitial-type, $a_0/3$<1 1 1> Frank loops using the inside/outside contrast method. It would appear that small loops at 1130 °C were also Frank loops: at least we confirmed the habit plane was {1 1 1} and their Burgers vector was parallel to <1 1 1>. The majority of those remained Frank loops even at 1460 °C: unfaulting of Frank loops was unfavorable at these irradiation conditions.

At irradiation temperature of 1130 °C, narrow loop DZ at a grain boundary implied that the being of invisible cavities which responsible for high sink strength for point defects. Rapid loop growth and density decrease were observed in the temperature range of 1300–1460 °C concurrently with the rapid cavity growth. The invisible cavities may also responsible for the slow growth speed of dense loops at or below the temperature.

Acknowledgements

The authors acknowledge fruitful discussions with Professor S. Golubov and Dr Y. Matsukawa. We would like to thank Dr F.W. Wiffen for reviewing the manuscript. This research was sponsored by the Office of Fusion Energy Sciences, US Department of Energy under contract DE-AC05-00OR22725 with UT-Battelle, LLC.

References

[1] Y. Katoh, L.L. Snead Jr., C.H. Henager, A. Hasegawa, A. Kohyama, B. Riccardi, H. Hegeman, J. Nucl. Mater. 367–370 (2007) 659.
[2] R.J. Price, J. Nucl. Mater. 48 (1973) 47.
[3] S. Kondo, T. Hinoki, A. Kohyama, Mater. Trans. 46 (2005) 1923.
[4] R.J. Price, J. Nucl. Mater. 33 (1969) 17.
[5] R. Blackstone, E.H. Voice, J. Nucl. Mater. 39 (1971) 319.
[6] L.L. Snead, Y. Katoh, S. Connery, J. Nucl. Mater. 367–370 (2007) 677.
[7] L.L. Snead, T. Nozawa, Y. Katoh, T.S. Byun, S. Kondo, D.A. Petti, J. Nucl. Mater. 371 (2007) 329.
[8] S.D. Harrison, J.C. Corelli, J. Nucl. Mater. 99 (1981) 203.
[9] T. Suzuki, T. Maruyama, T. Iseki, T. Mori, M. Ito, J. Nucl. Mater. 149 (1987) 334.
[10] T. Yano, T. Suzuki, T. Maruyama, T. Iseki, J. Nucl. Mater. 155–157 (1988) 311.
[11] T. Iseki, T. Maruyama, T. Yano, T. Suzuki, T. Mori, J. Nucl. Mater. 170 (1990) 95.
[12] D.J. Senor, G.E. Youngblood, L.R. Greenwood, D.V. Archer, D.L. Alexander, M.C. Chen, G.A. Newsome, J. Nucl. Mater. 317 (2003) 145.
[13] Y. Katoh, N. Hashimoto, S. Kondo, L.L. Snead, A. Kohyama, J. Nucl. Mater. 351 (2006) 228.
[14] T. Yano, T. Iseki, Philo. Mag. A 62 (1990) 421.
[15] T. Yano, H. Miyazaki, M. Akiyoshi, T. Iseki, J. Nucl. Mater. 253 (1998) 78.
[16] T. Suzuki, T. Yano, T. Maruyama, T. Iseki, T. Mori, J. Nucl. Mater. 165 (1989) 247.
[17] http://www.rohmhaas.com/.
[18] P.B. Hirsch, A. Howie, R.B. Nicholson, D.W. Pashley, M.J. Whelan, Electron Microscopy of Thin Crystals, Butterworth, London, 1965.
[19] H. Itoh, N. Hayakawa, I. Nashiyama, E. Sakuma, J Appl. Phys. 66 (1989) 4529.
[20] A. Kawasuso, H. Itoh, N. Morishita, M. Yoshikawa, T. Ohshima, I. Nashiyama, S. Okada, H. Okumura, S. Yoshida, Appl. Phys. A 67 (1998) 209.
[21] D.M. Follstaedt, Appl. Phys. Lett. 62 (1993) 1116.
[22] D.J. Eaglesham, A.E. White, L.C. Feldman, N. Moriya, D.C. Jacobson, Phys. Rev. Lett. 70 (1993) 1643.
[23] E.I. Givargizov, In Growth of Crystal, vol. 11, p.136 (1979 translated to English).
[24] H.L. Heinisch, L.R. Greenwood, W.J. Weber, R.E. Williford, J. Nucl. Mater. 327 (2004) 175.
[25] P.J.H. Denteneer, W. van Haeringen, J. Phys. C; Solid State Phys. 20 (1987) L883.
[26] L. Wang, H. Wada, L.F. Allard, J. Mater. Res. 7 (1992) 148.
[27] P. Käckel, J. Furthmüller, F. Bechstedt, Phys. Rev. B 58 (1998) 1326.
[28] Ulf Lindefelt, H. Iwata, S. Öberg, P.R. Briddon, Phys. Rev. B 67 (2003) 155204.
[29] M. Balarin, Phys. Stat. Sol. 11 (1965) K67.
[30] Y. Katoh, H. Kishimoto, A. Kohyama, J. Nucl. Mater. 307–311 (2002) 1221.
[31] L.L. Snead, R. Scholz, A. Hasegawa, A. Frias Rebelo, J. Nucl. Mater. 307–311 (2002) 1141.
[32] F. Gao, E.J. Bylaska, W.J. Weber, L.R. Corrales, Phys. Rev. B 64 (2001) 245208.
[33] J. Li, L. Porters, S. Yip, J. Nucl. Mater. 255 (1998) 139.
[34] B.L. Eyre, Fundamental Aspects of Radiation Damage in Metals, vol. 2, NTIS, Springfield, VA, 1975. p.729.
[35] H.R. Brager, F.A. Garner, E.R. Gilbert, J.E. Flinn, W.G. Wolfer, in: Radiation Effects in Breeder Reactor Structural Materials, TMS-AIME, New York, 1977. p. 727.
[36] B.N. Singh, A.J.E. Foreman, Philos. Mag. 29 (1974) 847.
[37] S.J. Zinkle, ASTM, Philadelphia, PA 19103 (1993) 749.
[38] L.K. Mansur, Nucl. Technol. 40 (1978) 5.

[39] L.K. Mansur, M.H. Yoo, J. Nucl. Mater. 85 & 86 (1979) 523.
[40] A.D. Brailsford, R. Bullough, Phys. Trans. Roy. Soc. 302 (1981) 87.
[41] S.J. Zinkle, in: R.E. Stoller, A.S. Kumar, D.S. Gelles (Ed.), Proceedings of the 15th International Symposium On Effects of Radiation on Materials, ASTM STP 1125, American Society for Testing and Materials, Philadelphia, 1992, p.749.
[42] L.W. Hobbs, A.E. Hughes, D. Pooley, Proc. Roy. Soc. A332 (1973) 167.
[43] L.W. Hobbs, F.W. Clinard Jr., S.J. Zinkle, R.C. Ewing, J. Nucl. Mater. 216 (1994) 291.
[44] S. Kondo, Y. Katoh, A. Kohyama, in: E. Lara-Curzio (Ed.), Mechanical Properties and Performance of Engineering Ceramics and Composites III, American Ceramic Society, 2007, p. 91.